Design of high-gain, wideband antenna using microwave hyperbolic metasurface

Yan Zhao[a]
International School of Engineering, Faculty of Engineering, Chulalongkorn University, Bangkok 10330, Thailand

(Received 5 April 2016; accepted 16 May 2016; published online 23 May 2016)

In this work, we apply hyperbolic metasurfaces (HMSs) to design high-gain and wideband antennas. It is shown that HMSs formed by a single layer of split-ring resonators (SRRs) can be excited to generate highly directive beams. In particular, we suggest two types of the SRR-HMS: a capacitively loaded SRR (CLSRR)-HMS and a substrate-backed double SRR (DSRR)-HMS. Both configurations ensure that the periodicity of the structures is sufficiently small for satisfying the effective medium theory. For the antenna design, we propose a two-layer-stacked configuration for the 2.4 GHz frequency band based on the DSRR-HMS excited by a folded monopole. Measurement results confirm numerical simulations and demonstrate that an antenna gain of more than 5 dBi can be obtained for the frequency range of 2.1 - 2.6 GHz, with a maximum gain of 7.8 dBi at 2.4 GHz. [http://dx.doi.org/10.1063/1.4952752]

I. INTRODUCTION

The first investigation of materials with simultaneously negative permittivity and permeability dates back to 1968.[1] However, due to the difficulty in their practical realization, such materials did not gain much attention until in 2000, Sir John Pendry proposed a concept of 'perfect lens',[2] which has an unlimited subwavelength resolution. Since then, the analysis of such artificial periodic structures with extraordinary electromagnetic properties that cannot be found in nature, termed as metamaterials (MMs), have attracted tremendous research interests. Notable applications of MMs include super-resolution imaging,[2,3] cloaking,[4] and perfect wave absorption[5] etc. More recently, a subcategory of MM, the so-called hyperbolic metamaterials (HMMs) whose isofrequency surface is a hyperboloid, have gained considerable attention as they support waves with unbounded wavevectors. Hyperbolic metasurfaces (HMSs), similar to their bulk counterpart, have also been shown to possess exceptional abilities to control the flow of light, achieve anomalously large photonic density of states, and super-resolution imaging.[6]

The applications of MM structures to antenna designs have long been investigated along with the development of MMs.[7,8] However, early designs require bulk MM structures which pose challenges in their practical realization.[9] The recent development of metasurfaces[10] has brought wide interests in their applications in antenna designs lately.[11–16] In this paper, based on our previous investigations on the generation of nondiffracting beams from HMSs,[17] we propose a two-layer-stacked antenna design using HMS for the 2.4 GHz frequency band, and demonstrate through numerical simulations and experiments that high antenna gain and wide bandwidth can be achieved. In contrast to the previous metasurface-antennas in which the metasurfaces act as impedance matching structures or parasitic radiating elements to enhance the antenna bandwidth,[11,12] the operation of our HMS design relies on altering wave vectors' directions;[17] comparing with metasurface-based leaky-wave antennas,[13–16] our proposed HMS antenna offers a smaller overall thickness and higher tolerance in fabrication. It is also worth mentioning that most of the research efforts have been put into the investigation of HMSs in

[a]yan.z@chula.ac.th

optical wavelengths; at microwave frequencies, such low-profile structures may find more attractive applications such as the construction of compact antennas, microwave absorbers and thin cloaks etc.

II. TRANSMISSION THROUGH HMS

Here we consider a transversely positive HMS[6] with its permittivity and permeability tensor specified as

$$\varepsilon = \varepsilon_0, \quad \mu = \mu_0 \begin{pmatrix} \mu_x & 0 & 0 \\ 0 & \mu_y & 0 \\ 0 & 0 & \mu_z \end{pmatrix}, \tag{1}$$

where $\mu_x = \mu_z > 0$ and $\mu_y < 0$. As shown in Fig. 1(a), the HMS is infinite along x- and z-directions, and its left boundary is aligned with the x-axis. The thickness of the HMS is L.

Following,[17] the electric field at any location (x, y) can be approximated as

$$E_z(x,y) \doteq E_0 \sum_{k_x} a_{k_x} e^{-jk_x(x-x_i)} \cdot \begin{cases} e^{-jk_y(y-y_i)} + Re^{jk_y(y+y_i)}, & y < 0, \\ Ae^{-j\kappa_y(y-y_i)} + Be^{j\kappa_y(y+y_i)}, & 0 \le y \le L, \\ Te^{-jk_y(y-y_i-L)}, & y > L, \end{cases} \tag{2}$$

where a_{k_x} is the amplitude of each Fourier component, and (x_i, y_i) is the location of the line source. The transmission and reflection coefficients, T and R are given by

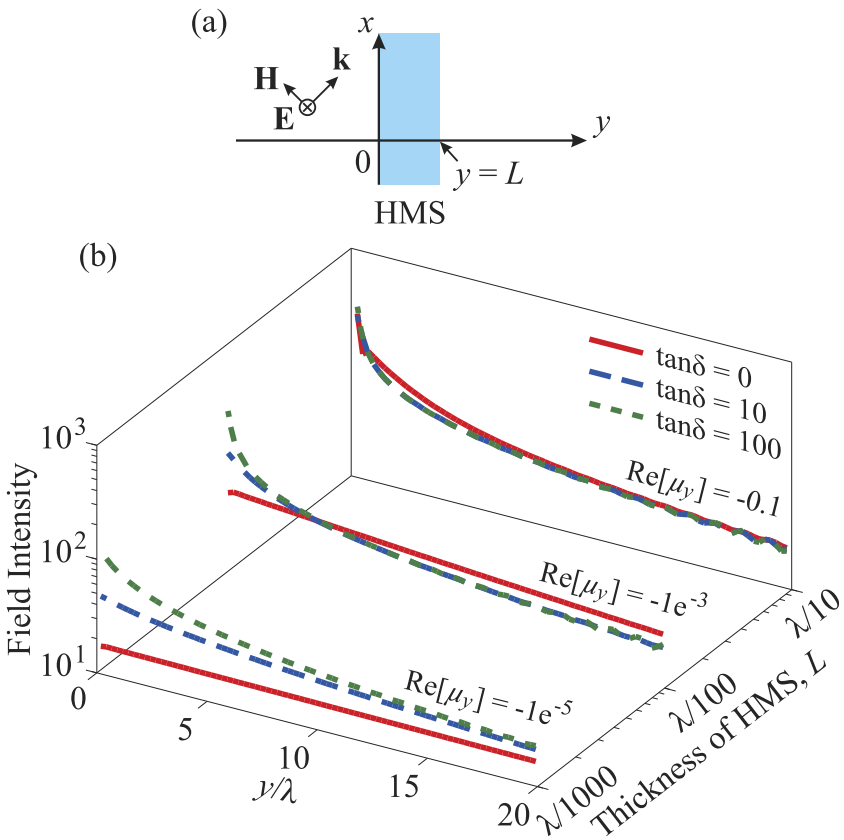

FIG. 1. (a) The two-dimensional domain for the transmission analysis of HMS. (b) The variations of electric field intensity along the y-direction for different thicknesses and amount of losses of HMS. In all cases, $\mu_x = 1$.

$$T = \frac{2\kappa_y k_y}{2\kappa_y k_y \cos(\kappa_y L) + j(\kappa_y^2 + k_y^2)\sin(\kappa_y L)}, \tag{3}$$

$$R = \frac{-j\sin(\kappa_y L)(\kappa_y^2 - k_y^2)}{2\kappa_y k_y \cos(\kappa_y L) + j(\kappa_y^2 + k_y^2)\sin(\kappa_y L)}, \tag{4}$$

and A and B can be calculated from T and R as

$$A = \frac{(1+R)e^{j\kappa_y L} - T}{2j\sin(\kappa_y L)}, \qquad B = \frac{(1+R)e^{-j\kappa_y L} - T}{-2j\sin(\kappa_y L)}, \tag{5}$$

where κ_y is given by the dispersion relation for the HMS (assuming $k_z = 0$):

$$\frac{k_x^2}{\mu_y} + \frac{\kappa_y^2}{\mu_x} = k_0^2. \tag{6}$$

Figure 1(b) shows the calculated variations of electric field intensity along the y-direction from Eq. (2) for different thicknesses and amount of losses of HMS. It can be seen that when the thickness is small (i.e. $L < \lambda/100$), for the lossless case (or small loss), the electric field intensity decays slowly with distance (red-solid lines), demonstrating a nondiffracting nature of waves and indicating that this type of HMS can be used to generate highly directive beams. When the amount of losses increases, although the transmitted field intensity increases accordingly due to the loss-enhanced transmission effect,[17] the waves after passing through HMS diverge rapidly. Such effect become more pronounced for HMSs with larger thicknesses. Thus it can be concluded that HMSs with small thicknesses are suited for designing highly directive antennas.

III. DESIGN OF MICROWAVE HMS USING SRR

As the essential requirement for designing HMS at microwave frequencies is to have near zero and negative permeability along the longitudinal direction, and positive permeability (≈ 1) in transverse directions, the co-planar SRR structure is a suited candidate for realizing the homogeneous HMS slab for transverse electric (TE) field illuminations (with respect to the surface of SRR). Here we consider two types of the SRR structure: an array of capacitively-loaded single SRRs (CLSRRs) and an array of substrate-backed double SRRs (DSRRs). The geometries and dimensions of the structures are shown in Figs. 2(a) and 2(b). A plane-wave analysis is performed using the finite element method (FEM) to retrieve the effective permeability of the structures.[18] In the analysis, the standard configuration for permeability retrieval as detailed in Ref. 18 is considered, and the transverse electromagnetic (TEM) wave is used as excitation with the magnetic field aligned perpendicular to the plane of the SRR. However, it is important to note that the retrieved permeability only provides a guidance for tuning the SRR structure, since in our HMS design, the SRRs are arranged in a co-planar fashion. The extracted relative permeability for the single-layer CLSRR and DSRR structures is shown in Figs. 2(c) and 2(d), respectively. In order to satisfy the effective medium theory and guarantee accuracy in permeability retrieval, the dimensions of the unit cell should be sufficiently small comparing to the wavelength. Therefore the capacitors in the CLSRR-HMS and the substrate and double-ring design for the DSRR-HMS are introduced to reduce the sizes of unit cells. As it is shown in Figs. 2(c) and 2(d), negative and near zero values of $\mathrm{Re}(\mu_y)$ can be obtained at slightly below 2.5 GHz for both CLSRR-HMS and DSRR-HMS.

Figures 2(e) and 2(f) show the FEM calculated distributions of electric field intensity for the CLSRR-HMS and DSRR-HMS, respectively. In both cases, an electric line-source along the z-direction is placed at a distance of $\lambda/30$ from the HMS and used as excitation, and the periodic boundary conditions (PBCs) are applied along the z-direction to model infinite structures. The transverse dimension of both HMSs is 3λ, which is large enough to avoid corner diffractions.[17] A perfect electric conductor (PEC) is placed at a distance of $\lambda/20$ at the back of the line source as a reflector. For both structures, the dimensions of the SRRs are varied such that the distributions with the highest spatial confinement of electric field are obtained at 2.45 GHz. It is evident that the electric field is

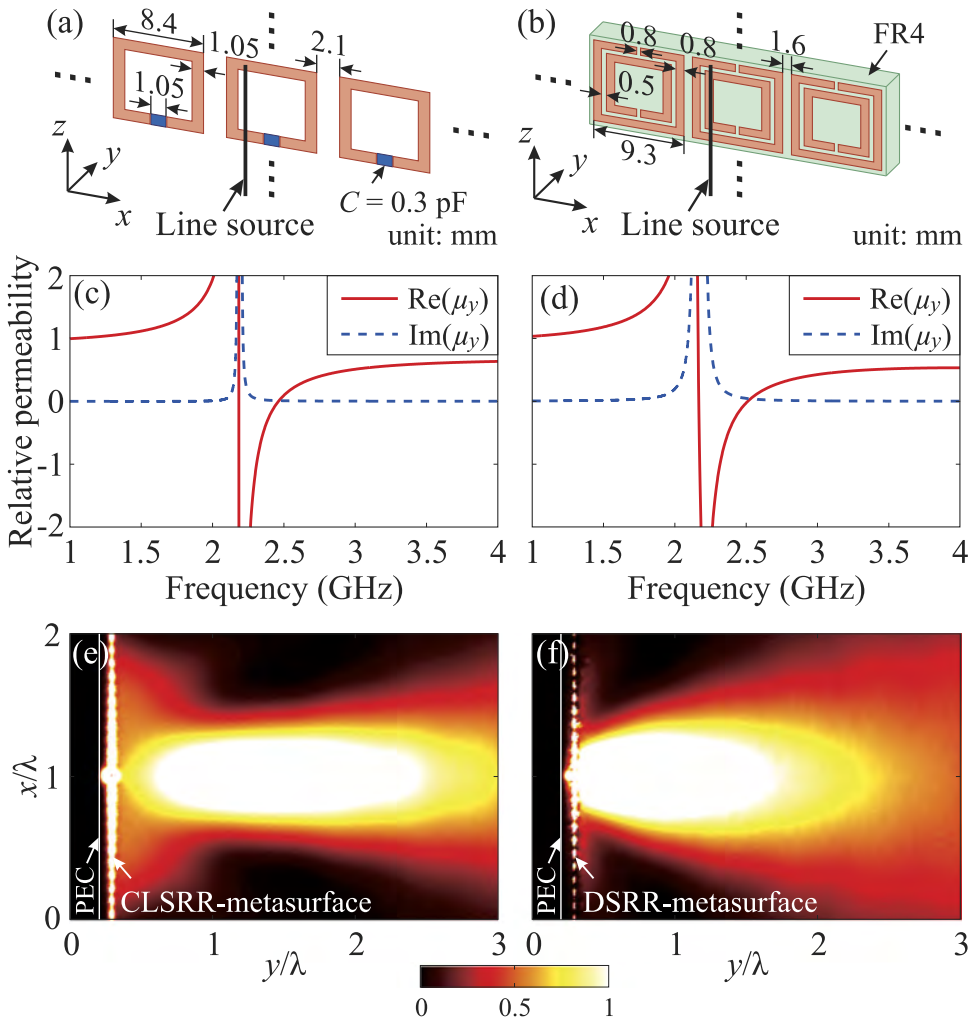

FIG. 2. Microwave metasurfaces formed by a single layer of (a) capacitively loaded SRRs (CLSRRs), and (b) substrate-backed double SRRs (DSRRs). Retrieved effective permeability for (c) the CLSRR-HMS, and (d) the DSRR-HMS. Distributions of electric field intensity for (e) the CLSRR-HMS and (f) the DSRR-HMS, both at 2.45 GHz.

more spatially confined (or directive) for the CLSRR-HMS, which is due to the fact that the effective thickness of the CLSRR-HMS is much smaller than that of the DSRR-HMS. In addition, the CLSRR-HMS is less lossy observed from the imaginary part of the extracted permeability, owing to its simpler composition with less metallic part. It is worth mentioning that there exist spatial dispersion effects in SRR structures. However, such effects do not play an important role in generating highly directive beams from HMS, and the HMS behaves as a wave vector redirecting device. Although the above results show that more directive beams can be generated for structures with smaller unit cells, the DSRR-HMS offers an easier fabrication process and more stable performance. In the following section, we propose an antenna design for the 2.4 GHz frequency band based on the DSRR-HMS.

IV. DESIGN OF HIGH-GAIN AND WIDEBAND ANTENNA USING DSRR-HMS

The proposed antenna has a two-layer-stacked configuration, as shown in Fig. 3(a). The first layer is a folded monopole above a ground plane (with a gap in between), for generating TE-polarized waves (with respect to the ground plane). The second layer is a DSRR-HMS on a substrate. Figure 3(d) shows the retrieved effective permeability of the DSRR-HMS. It can be seen that the desired permeability of being negative and near zero along the longitudinal direction can be obtained at frequencies

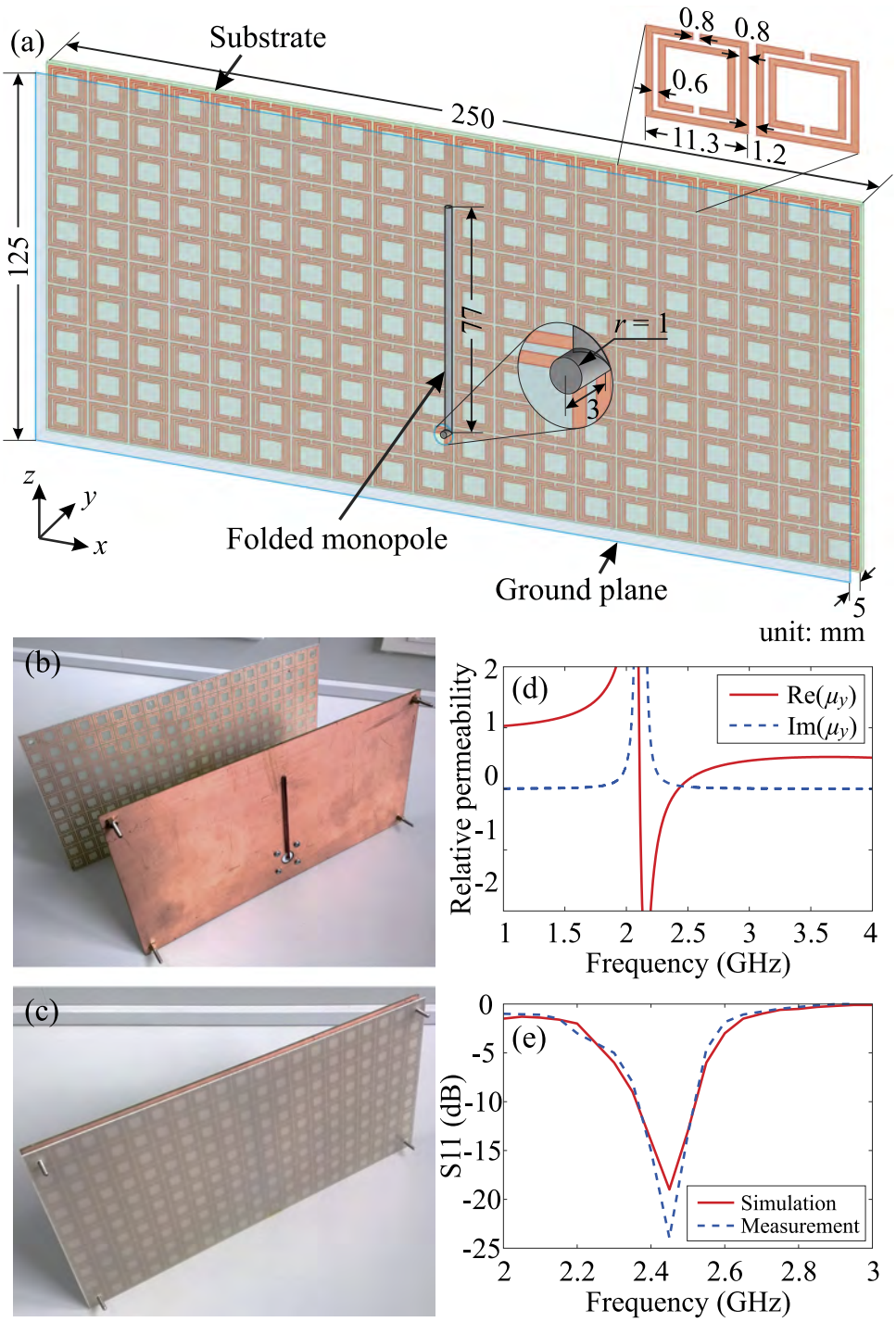

FIG. 3. (a) The configuration of the proposed antenna consisting of a DSRR-HMS and a folded monopole above a ground plane. (b) The fabricated DSRR-HMS and the folded monopole. (c) The complete antenna after two layers are assembled together. (d) The retrieved effective permeability of the DSRR-HMS. (e) Comparison of simulated and measured return loss of the antenna.

below 2.5 GHz. The antenna is simulated using FEM, and the dimensions of the folded monopole and DSRR-HMS are optimized for tuning and achieving the maximum directivity of the antenna at 2.4 GHz. Then the design is fabricated on two single-sided printed circuit boards (PCBs) on FR4 substrates. The connector used in the design is a panel-mount N-type female connector with 50 Ohm

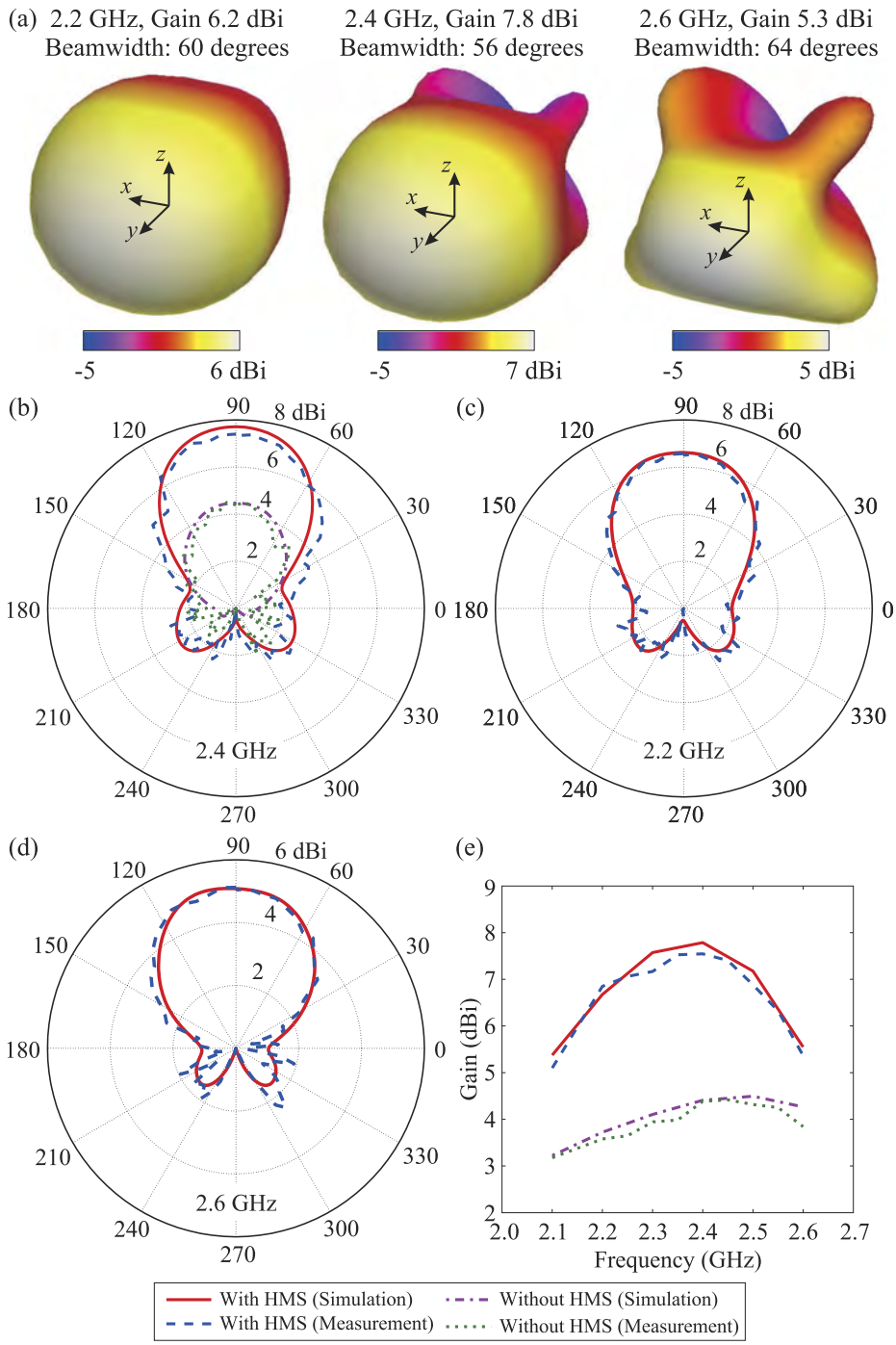

FIG. 4. (a) The radiation patterns of the proposed antenna at 2.2, 2.4 and 2.6 GHz from FEM simulations. (b) Comparison between simulated radiation patterns and measurement results at 2.4 GHz in the x-y plane for the cases of with and without the use of the DSRR-HMS. Comparison between simulated and measured radiation patterns at (c) 2.2 GHz and (d) 2.6 GHz with the use of the DSRR-HMS. (e) Comparison between simulated and measured antenna gain in the frequency range of 2.1 - 2.6 GHz.

impedance. The fabricated antenna before and after the two layers are assembled is shown in Figs. 3(b) and 3(c), respectively. A spacer screw of 5 mm in length is used to separate the PCBs, and the copper side of the DSRR-HMS faces the monopole. The comparison between simulated and measured return loss (S_{11}) is plotted in Fig. 3(e) and shows a good impedance matching of the antenna.

Figure 4(a) shows the radiation patterns at 2.2, 2.4 and 2.6 GHz from FEM simulations, with the highest gain of 7.8 dBi at 2.4 GHz. The antenna has a stable 3 dB-beamwidth of around 60 degrees across the frequency band, and an increasing level of sidelobes at higher frequencies. The efficiency of the antenna is found from simulations to be between 85% and 90% at the above frequencies. The radiation patterns (gain) of the fabricated antenna in the x-y plane (see Fig. 3(a)) are measured in an anechoic chamber using a vector network analyzer (VNA) Rohde & Schwarz ZVB20 in the frequency range of 2.1 - 2.6 GHz, by the gain comparison method using a standard horn antenna with the working frequencies of 800 MHz to 18 GHz (model R&S HF907). Figure 4(b) shows the comparison of gain patterns from simulations and measurement at 2.4 GHz with and without the use of the DSRR-HMS. The gain patterns of the antenna at 2.2 and 2.6 GHz are shown in Figs. 4(c) and 4(d), respectively. The comparison between simulated and measured gain in the frequency range of 2.1 - 2.6 GHz is shown in Fig. 4(e). It can be seen that when the DSRR-HMS is used, the maximum gain across the frequency band is increased from 4.2 to 7.8 dB, with a 3.6 dB enhancement. Moreover, there is a slight frequency shift for the maximum gain due to the introduction of the DSRR-HMS. Comparing with other antenna designs, for example, antenna arrays with the same aperture size, although they offer higher gain of over 10 dBi, a separate feeding network is necessary; on the other hand, our proposed design allows easy fabrications. In contrast to Fabry-Perot cavity-based antennas and antennas with superstrate made from artificial magnetic conductors (AMCs), despite their capability of providing higher gain enhancement, they require the distance between the superstrate and the feeding element to be equal to $\lambda/2$ and $\lambda/4$, respectively; our design allows the HMS to be placed in close proximity ($\lambda/25$), and hence leading to a low profile of the antenna.

V. CONCLUSION

It is shown that highly directive beams can be generated from HMSs and such effects are more pronounced for thin HMSs. For the realization of HMS, we suggest two configurations, namely the CLSRR-HMS and the DSRR-HMS. Results show that both structures can be used to generate spatially confined beams to free space. In the antenna design, we propose a two-layer-stacked configuration consisting of a folded monopole for excitation and a single layer of DSRR-HMS for generating highly directive waves. Measurement results confirm numerical simulations and show that a maximum gain of 7.8 dBi can be obtained at the design frequency of 2.4 GHz, and a more than 5 dBi gain can be achieved over the frequency range of 2.1 - 2.6 GHz. The proposed antenna design may find its applications in indoor WiFi basestations.

ACKNOWLEDGMENT

This research was funded by the Ratchadapisek Sompoch Endowment Fund (2014), Chulalongkorn University (CU-57-035-AM). The author acknowledges King Mongkut's University of Technology North Bangkok (KMUTNB) for providing antenna measurement facilities.

[1] V. G. Veselago, "The electrodynamics of substances with simultaneously negative values of ε and μ," Sov. Phys. Usp. **10**, 509 (1968).
[2] J. Pendry, "Negative refraction makes a perfect lens," Phys. Rev. Lett. **85**, 3966 (2000).
[3] N. Fang, H. Lee, C. Sun, and X. Zhang, "Sub-diffraction-limited optical imaging with a silver superlens," Science **308**, 534 (2005).
[4] J. B. Pendry, D. Schurig, and D. R. Smith, "Controlling electromagnetic fields," Science **312**, 1780 (2006).
[5] N. I. Landy, S. Sajuyigbe, J. J. Mock, D. R. Smith, and W. J. Padilla, "Perfect metamaterial absorber," Phys. Rev. Lett. **100**, 207402 (2008).
[6] A. V. Kildishev, A. Boltasseva, and V. M. Shalaev, "Planar photonics with metasurfaces," Science **339**, 1232009 (2013).
[7] R. W. Ziolkowski, P. Jin, and C.-C. Lin, "Metamaterial-inspired engineering of antennas," Proc. IEEE **99**(10), 1720-1731 (2011).
[8] Y. Dong and T. Itoh, "Metamaterial-based antennas," Proc. IEEE **100**(7), 2271-2285 (2012).
[9] B.-I. Wu, W. Wang, J. Pacheco, X. Chen, T. M. Grzegorczyk, and J. A. Kong, "A study of using metamaterials as antenna substrate to enhance gain," Prog. Electromagn. Res. **51**, 295-328 (2005).
[10] C. L. Holloway, E. F. Kuester, J. A. Gordon, J. O'Hara, J. Booth, and D. R. Smith, "An overview of the theory and applications of metasurfaces: The two-dimensional equivalents of metamaterials," IEEE Antennas Propag. Mag. **54**(2), 10-35 (2012).
[11] K. L. Chung and S. Chaimool, "Broadside gain and bandwidth enhancement of microstrip patch antenna using a MNZ-metasurface," Microw. Opt. Techn. Lett. **54**(2), 529-532 (2012).

[12] S. Chaimool, C. Rakluea, and P. Akkaraekthalin, "Mu-near-zero metasurface for microstrip-fed slot antennas," Appl. Phys. A **112**, 669-675 (2013).
[13] A. Mehdipour, J. W. Wong, and G. V. Eleftheriades, "Beam-squinting reduction of leaky-wave antennas using Huygens metasurfaces," IEEE Trans. Antennas. Propag. **63**(3), 978-992 (2015).
[14] D. Blanco, E. Rajo-Iglesias, S. Maci, and N. Llombart, "Directivity enhancement and spurious radiation suppression in leaky-wave antennas using inductive grid metasurfaces," IEEE Trans. Antennas. Propag. **63**(3), 891-900 (2015).
[15] S. Pandi, C. A. Balanis, and C. R. Birtcher, "Design of scalar impedance holographic metasurfaces for antenna beam formation with desired polarization," IEEE Trans. Antennas. Propag. **63**(7), 3016-3024 (2015).
[16] C. Pfeiffer and A. Grbic, "Planar lens antennas of subwavelength thickness: Collimating leaky-waves with metasurfaces," IEEE Trans. Antennas. Propag. **63**(7), 3248-3253 (2015).
[17] Y. Zhao, "Nondiffracting beam emission from hyperbolic metasurfaces," J. Opt. **17**, 045103 (2015).
[18] D. R. Smith, S. Schultz, P. Markos, and C. M. Soukoulis, "Determination of effective permittivity and permeability of metamaterials from reflection and transmission coefficients," Phys. Rev. B. **65**, 195104 (2002).